

Evaluation of static response in stress-ribbon concrete pedestrian bridges

Leonidas T. Stavridis[†]

*Structural Engineering, National Technical University of Athens, Vas. Sofias 100-11528
Athens, Greece*

(Received January 15, 2009, Accepted October 6, 2009)

Abstract. An analytical method is proposed for the evaluation of the static response of a prestressed-ribbon concrete pedestrian bridge, which may also be applied for the roofing of large areas. On the basis of an established analogy with a suspension bridge system, a procedure is presented for the prestressed-ribbon direct analysis, leading to the introduction of two dimensionless parameters as governing factors of the design, namely the thinness and the prestressing steel ratio. The exposed procedure, applied by a simple computer program, allows a quick evaluation of the response and permits the investigation of the influence of the aforementioned parameters on it, by means of comprehensive diagrams. The presented diagrams may be directly used for the preliminary design of a pedestrian bridge of this type, for the whole practical range of span lengths. A design example is also included, showing the applicability of the proposed procedure.

Keywords: stress-ribbon; bridge; suspension bridge; static analysis; design.

1. Introduction

The cable has always been recognized as the most efficient load-bearing element from a point of view of strength exploitation, because of the automatic adoption of the funicular form for any loading pattern, however with two serious drawbacks, namely the need to anchor the high cable forces on one hand and the need to restrict the excessive deformability due to additional load on the other. The first problem is usually tackled with means that practically do not interact directly with the load-bearing action of the cable itself, while the second one has been surpassed by implementing a horizontal girder which, for any additional (live) loading, restricts the cable deformability decisively, by its appropriately chosen bending stiffness.

This same problem has been addressed the last twenty years regarding mainly pedestrian bridges, in a constructionally different and aesthetically very satisfactory way, through the so called stress ribbon construction.

The stress-ribbon concept consists in embedding a hanging cable in a relatively thin band of concrete and then, through additional (pre)stressing of the cable, setting the so created inverted concrete arch under uplift pressures, which cause a compressive state of stress in the arch. In this

[†] Associate Professor, E-mail: stavrel@central.ntua.gr

way, additional live loads applied later can be taken up without excessive deformation of the cable, thanks to the effective bending rigidity of the arch acquired through its compressive state of stress. Although such a structural system can also be applied for the covering of large areas, it has been established rather in its use for pedestrian bridge projects.

A drawback of this structural system is surely the high cable forces, due to the low sag-to-span ratio, which need to be anchored, but on the other side, the resulting exceptional slenderness of these structures, allows them to adjust in the environment in a very satisfactory way.

Concerning the structural analysis, the governing factor which has to be appropriately taken into account is the geometric non-linearity of the behavior, arising from the interaction of the concrete ribbon with the cable itself. Moreover, creep effects due to the higher concrete compression stresses, and possible vibrations that may be induced by the pedestrians, have also to be taken into account in the design of stress-ribbon concrete bridges.

The publications that have appeared on this subject refer not only to its theoretical aspects but also to the special characteristics and problems encountered in the realization of such bridge projects.

In (Redfield and Strasky 1991), on the occasion of the first use of this type of structure for a footbridge in the United States, the basic structural principles and their consequences for the construction method used are shown, together with the exposition of the main issues of the static and dynamic analysis involved. An interesting and comprehensive review of all the relevant design and analytical aspects involved in stress-ribbon pedestrian bridges, is given in (Schlaich and Engelsmann 1996). Furthermore, a systematic analytic examination of the most important behavioral aspects of the structural problem is given more recently in (Arco *et al.* 2001), where the time-dependent effects and the vertical vibration characteristics are also included.

In the present paper, an original analytical method is presented for the direct evaluation of the overall static response of a stress-ribbon structure - used mainly as pedestrian bridge - under the action of live loads, based on an established analogy with the suspension bridge behavior, as it has been exposed by the author in (Stavridis 2008). Following this analogy, the analysis of the stress-ribbon system is carried out by the use of three dimensionless parameters which, for a given span length, are appropriately expressed on the basis of two selected design parameters, namely the ratio of the ribbon thickness over the span length and the ratio of the section area of the prestressing cables over the concrete section. The analysis is performed through an efficient numerical procedure which, by means of a simple computer program, allows the immediate evaluation of the response of the system due to the imposed live load. Moreover the procedure enables a parametric study resulting in comprehensive diagrams which show the influence of the above design parameters on the overall static response, so that they may be used directly for preliminary design purposes.

2. Conceptual analogy and analysis

Whereas for roofing large areas the shallowness ratio of the cable i.e., sag-to-span ratio may lie in the range of 1/10, the use of such a ribbon as a pedestrian bridge poses automatically the restriction of maximum slope to 8%, which shows a shallowness ratio equal to 1/50.

In order to estimate the response of the arch, as well as that of the cable, due to an imposed additional live load, the combined action of the cable and the arch has to be taken into account. The fact that the common deflection of the cable and of the arch is determined both from the axial

rigidity of the cable and the bending rigidity of the arch itself, leads to the conclusion that this system behaves like a fictitious suspension system with separate cable and stiffening girder. Indeed, in such a system, after an initial geometry for the cable sag under permanent loads has been established through an appropriate cable force introduced, a later applied live load to the stiffening beam produces identical deflections to the cable and the girder at each point, thanks to the vertical hangers. It can be concluded that the stress-ribbon system exhibits the same characteristics as the suspension bridge and consequently, this model may be used as a fictitious model for the analysis of the system examined, assuming no bond between the cable and the surrounding concrete.

The cable profile is characterized by its prescribed sag f which, referring to span length L , determines the shallowness ratio λ

$$\lambda = \frac{f}{L} \tag{1}$$

as well as the curvature of the cable from the expression

$$\frac{1}{R} = \frac{8 \cdot \lambda}{L} \tag{2}$$

This sag is maintained not only through the self weight g of the concrete ribbon causing the initial cable force H_g , but also through an additional uniform downward load u_v , acting on the cable, as caused by the additional prestressing force H_v (Fig. 1(a)). It is

$$u_v = \frac{H_v}{R} \tag{3}$$

This means that the fictitious suspension system may be considered as having an initial permanent load w applied to the stiffening beam (Fig. 2), equal to

$$w = g + u_v \tag{4}$$

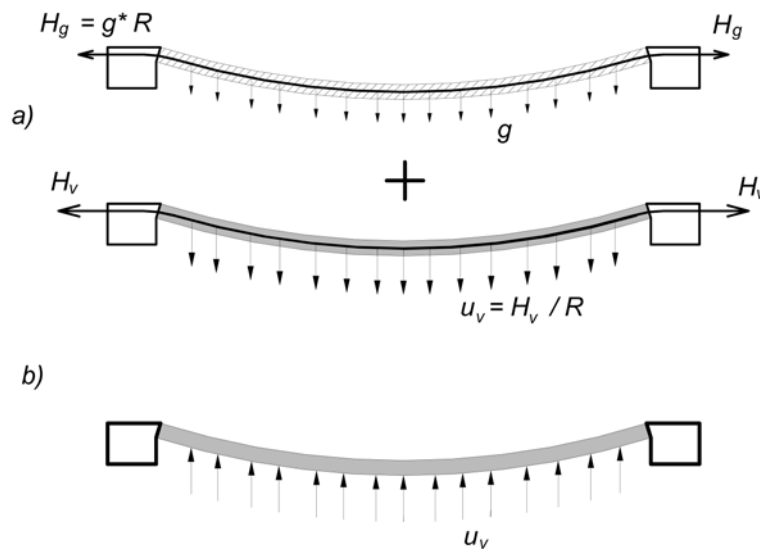


Fig. 1 System layout and prestressing (a) Initial actions on the cable (b) Initial actions on the inverted arch

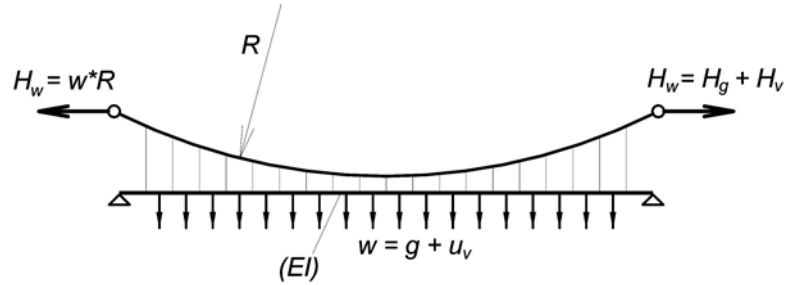


Fig. 2 Simulative suspension model under initial actions of permanent load and prestressing

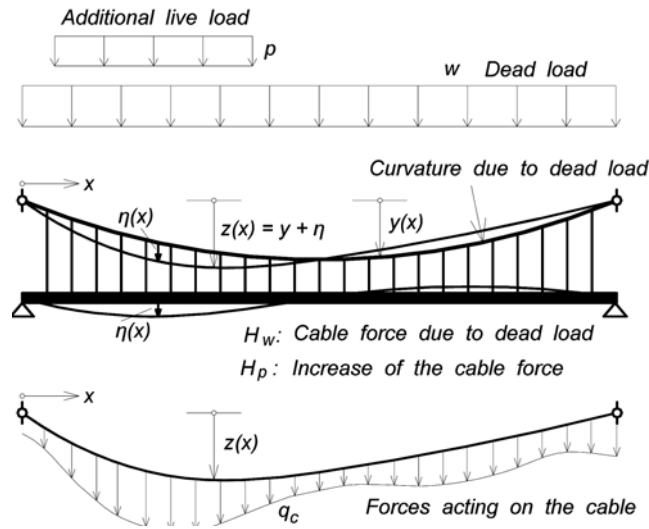


Fig. 3 Cable deformation in simulation model under direct action of live load

The stiffening role of the arch, ensured by the state of compression imparted to it by the upwards directed load u_v (Fig. 1(b)), corresponds to the analogous bending rigidity of the stiffening beam of the fictitious suspension system with the same cross section, expressed through the quantity (EI) , which refers to the orthogonal section $(b \times t)$ of the inverted arch, where b and t represent its unit width and thickness respectively.

After a live load p is applied on the fictitious girder over a specified length, the cable, having an initial profile $y(x)$, deflects – together with the girder - by $\eta(x)$, increasing its axial force by H_p (Fig. 3). The following expression describes the new geometry $z(x)$ of the cable

$$z(x) = y(x) + \eta(x) \quad (5)$$

and its vertical equilibrium requires a distributed force q_c acting on it downwardly and equal to

$$q_c(x) = -\frac{d^2z}{dx^2}(H_w + H_p) \quad (6)$$

where H_w represents the total initial cable force due to the permanent load w . It can be written

$$H_w = H_g + H_v = \frac{w \cdot L}{8 \cdot \lambda} \tag{7}$$

The total load acting on the girder is (Fig. 4(a))

$$q(x) = -q_c(x) + w + p \tag{8}$$

The girder deflection $\eta(x)$ has to obey the classical beam equation

$$EI \frac{d^4 \eta}{dx^4} = q(x) \tag{9}$$

that, on the basis of Eqs. (4), (5), (6) and by considering (d^2y/dx^2) as the negative cable curvature under the load w , it can be written

$$EI \frac{d^4 \eta}{dx^4} - \frac{d^2 \eta}{dx^2} (H_w + H_p) = p - \frac{H_p}{R} \tag{10}$$

This equation, representing the classical differential equation of the “deflection theory” of suspension bridges under a permanent load w , may be recognised (Stavridis 2008) as the equation of a simple beam having a transverse load equal to $(p - H_p/R)$ and subjected to an axial load equal to $(H_w + H_p)$, according to the second order theory of beams (Fig. 4(b)).

The increase H_p of the cable force, given the low shallowness ratio $\lambda = 0.02$, is related to its additional deflection η with good accuracy, through the relation

$$\frac{H_p}{A_c E_c} \times L \cdot (1 + 8 \times \lambda^2) = \frac{1}{R_0} \int \eta dx \tag{11}$$

It is understood that the unknown magnitude H_p can be determined from the condition that the deflection $\eta(x)$ of the tensioned beam according to Eq. (9), must also satisfy the “cable equation” (11).

The deflection $\eta(x)$ of a simple beam due to a transverse load q and subjected to a tensile force H (Fig. 5(a)), is obtained from the following expression (Timoshenko 1956)

$$\eta(x) = \frac{q}{H} \left[\frac{\cosh(k \cdot L/2 - k \cdot x)}{k^2 \cdot \cosh(k \cdot L/2)} - \frac{1}{k^2} + \frac{x \cdot (L-x)}{2} \right] \tag{12}$$

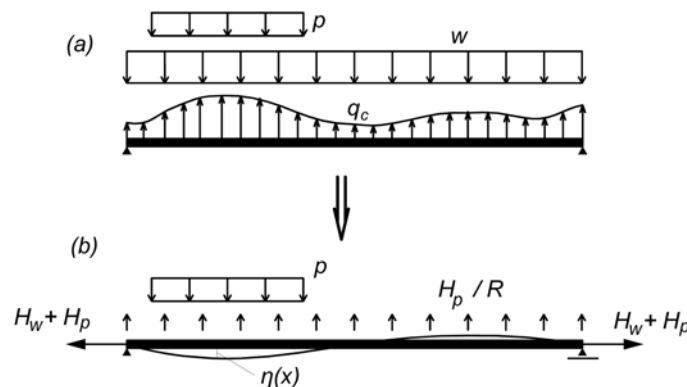


Fig. 4 Acting forces on the stiffening (a) and the fictitious, (b) beam of the simulative model

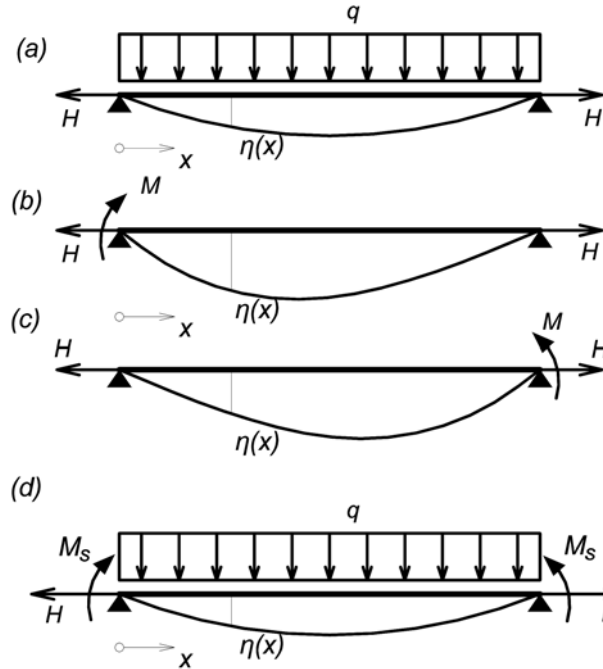


Fig. 5 Tensioned beam under transverse and end-moment loading

whereas due to a concentrated moment M at the left or at the right support (Fig. 5(b, c)), it is respectively

$$\eta(x) = \frac{M}{H} \left[\frac{L-x}{L} - \frac{\sinh(k \cdot L - k \cdot x)}{\sinh(k \cdot L)} \right] \quad \text{or} \quad \eta(x) = \frac{M}{H} \left[\frac{x}{L} - \frac{\sinh(k \cdot x)}{\sinh(k \cdot L)} \right] \quad (13)$$

with

$$k = \sqrt{\frac{H}{EI}} \quad (14)$$

The system of Eqs. (10) and (11) may be applied either for a two-hinged stiffening girder, or for a girder with fixed ends, corresponding to the actual boundary conditions of the stress-ribbon arch. It has to be noted that as a rule, the stress ribbon bridges are constructed with an established fixity at both ends, although the two-hinged arch leads to much more moderate bending response. The reason is that the cable over the hinges may be more prone to fatigue overstressing on one hand and, as it will be shown later, the deflections for the applied shallowness ratio (1/50), can be definitely greater. However, in the suspended beam model followed, the “hinged” case will be treated first, as it forms the basis for the numerical solution for the fixed stiffening girder.

According to (Stavridis 2008), the response of the suspension system is governed by three dimensionless parameters which are expressed as follows

$$G = \frac{H_w \times L^2}{E \cdot I}, \quad \gamma = \frac{p}{w}, \quad \varepsilon = \frac{H_w}{A_c \cdot E_c} \quad (15)$$

whereas the unknown parameter Z of the problem is

$$Z = \frac{H_p}{H_w} \tag{16}$$

In the above expressions H_w corresponds to the cable force under permanent loading w .

2.1 Hinged stiffening girder

In the case of hinged stiffening girder, the system of Eqs. (10) and (11) leads through Eq. (12) to the transcendental equation

$$Z \cdot \varepsilon \cdot (1 + 8 \cdot \lambda^2) = 64 \cdot \lambda^2 \cdot \frac{\gamma - Z}{Z + 1} \cdot \left[\frac{2 \cdot \sinh(D/2)}{D^3 \cdot \cosh(D/2)} - \frac{1}{D^2} + \frac{1}{12} \right] \tag{17}$$

with

$$D = \sqrt{G \times (Z + 1)} \tag{18}$$

The above equation is not directly solvable. However, by working out an approximate solution of the tensioned beam as mentioned above, it is found (Stavridis 2009) that the unknown parameter Z , in the case where the live load p extends over the whole span, can be determined with very satisfactory accuracy through the following quadratic equation

$$Z^2 + \left(\frac{\pi^2}{G} + \omega + 1 \right) \times Z - \gamma \times \omega = 0 \tag{19}$$

where

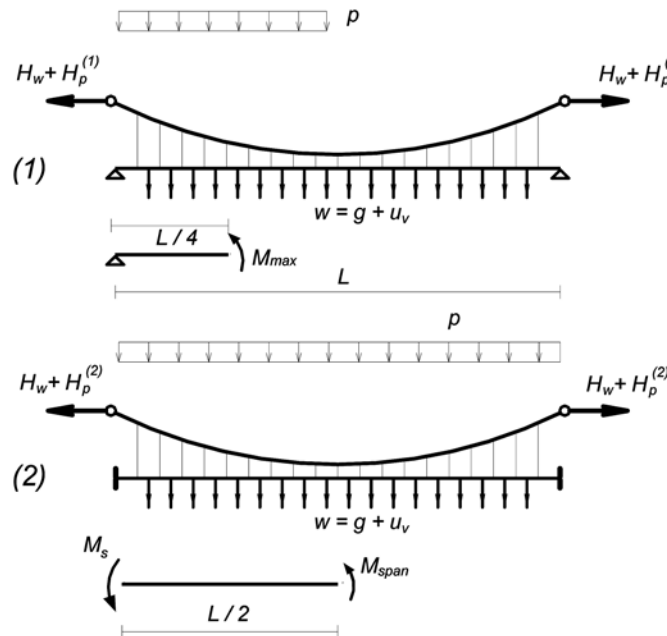


Fig. 6 Live load layout and respective bending response in simulation model for the hinged (1) and the fixed (2) case

$$\omega = \frac{8 \cdot \pi^2}{15 \times \varepsilon} \cdot \frac{1}{1/\lambda^2 + 8} \quad (20)$$

In order now to obtain the maximum bending response of the stiffening girder, the live load p must be placed over the half span length (Fig. 6(a)) and then, at the quarter of the span, the following expression is obtained

$$M_{\max} = \left\{ \frac{8 \cdot (\gamma - Z)}{D^2} \cdot \left[\frac{\cosh(D/4)}{\cosh(D/2)} - 1 \right] + \frac{8 \cdot \gamma}{D^2} \cdot \left[\frac{1}{\cosh(D/4)} - 1 \right] \right\} \times M_w^0 \quad (21)$$

where

$$M_w^0 = \frac{w \cdot L^2}{8} \quad (22)$$

whereas for the corresponding maximum deflection it is obtained

$$\frac{\eta_{\max}}{L} = \frac{8 \cdot \lambda \cdot (\gamma - Z)}{(Z + 1) \cdot D^2} \cdot \left[\frac{\cosh(D/4)}{\cosh(D/2)} + \frac{3 \cdot D^2}{32} - 1 \right] + \frac{8 \cdot \lambda \cdot \gamma}{(Z + 1) \cdot D^2} \cdot \left[\frac{1}{\cosh(D/4)} + \frac{D^2}{32} - 1 \right] \quad (23)$$

It has to be noted that the value of Z in the last expression corresponds to the one determined according to Eq. (19), by taking into account the half value of γ .

2.2 Stiffening girder with fixed ends

According to Eqs. (12), (13), the deflection of a simple beam subjected to an axial and a transverse load equal to H and q respectively, as well as to two equal end moments M_s (Fig. 5(d)), may be expressed as

$$\eta(x) = \frac{q}{H} \left[\frac{\cosh(k \cdot L/2 - k \cdot x)}{k^2 \cdot \cosh(k \cdot L/2)} - \frac{1}{k^2} + \frac{x \cdot (L - x)}{2} \right] + \frac{M_s}{H} \cdot \left[1 - \frac{\cosh(k \cdot L/2 - k \cdot x)}{k^2 \cdot \cosh(k \cdot L/2)} \right] \quad (24)$$

Determining the bending moments M_s from the condition of fixity ($d\eta/dx = 0$), under consideration of an axial and transverse load equal to $(H_w + H_p)$ and $(p - H_p/R)$ respectively, as well as of the Eqs. (15), (16), the following expressions are obtained

$$M_s = w \cdot L^2 \cdot \frac{\gamma - Z}{D^2} \cdot \left[1 - \frac{D}{2 \cdot \tanh(D/2)} \right] \quad (25)$$

and

$$\eta(x) = \frac{8 \cdot \lambda \cdot L}{D^2} \cdot \frac{\gamma - Z}{Z + 1} \cdot \left\{ \frac{\cosh(D/2 - D \cdot x/L)}{\cosh(D/2)} - 1 + \frac{D^2}{L^2} + \frac{x \cdot (L - x)}{2} \right. \\ \left. + \left[1 - \frac{D}{2 \cdot \tanh(D/2)} \right] \left[1 - \frac{\cosh(D/2 - Dx/L)}{\cosh(D/2)} \right] \right\} \quad (26)$$

By substituting now the above expression of $\eta(x)$ into the cable Eq. (11), the following equation for the determination of the unknown parameter Z is obtained

$$\frac{1}{8} \cdot Z \cdot \varepsilon \cdot \left(1 + \frac{1}{8 \cdot \lambda^2} \right) \cdot \frac{Z + 1}{\gamma - Z} = \frac{1}{D^2} - \frac{1}{2 \cdot D \cdot \tanh(D/2)} + \frac{1}{12} \quad (27)$$

This transcendental equation is not directly solvable. Nevertheless it is possible to obtain quickly an accurate solution by the method of successive approximations, if, as starting value Z_0 , is taken that one developed in the previously examined model of the hinged girder, according to Eq. (19).

It is important to note that the value of the solution Z of Eq. (26) is always less than Z_0 by no more than 8% and this fact makes the procedure of its accurate determination by the method of successive approximations, a very fast one.

On the basis of this value Z , the bending moment M_f at the fixed end of the girder is determined through Eq. (25), causing tension on its upper fibres (Fig. 6(b)).

The resulting bending moment M_{span} at the middle of the span can be readily obtained through the classical relation

$$M = -EI \cdot \frac{d\eta^2}{dx^2} \tag{28}$$

It is found

$$M_{span} = w \cdot L^2 \cdot \frac{\gamma - Z}{D^2} \cdot \left[1 - \frac{D}{2 \cdot \sinh(D/2)} \right] \tag{29}$$

Regarding the corresponding deflection at the middle of the span according to Eq. (26), it is

$$\frac{\eta_{(x=L/2)}}{L} = 8 \cdot \lambda \cdot \frac{\gamma - Z}{Z + 1} \cdot \left\{ \frac{2}{D^2} + \frac{1}{2 \cdot D \cdot \tanh(D/2)} \cdot \left[\frac{1}{\cosh(D/2)} - 1 \right] + \frac{1}{8} \right\} \tag{30}$$

However it has to be noted here that the upward pressure u_v on the arch from the cable following its prestressing (Fig. 1(b)), produces additionally a fixed-end bending moment M_{fix} , which causes tension to the bottom fibres of the arch (Fig. 7(a)) and depends practically only on its shallowness ratio λ and its thickness. (Schlaich *et al.* 1996). This bending moment, for the value $\lambda = 0.02$ in use, can be practically obtained from the following expression, with a satisfactory accuracy for

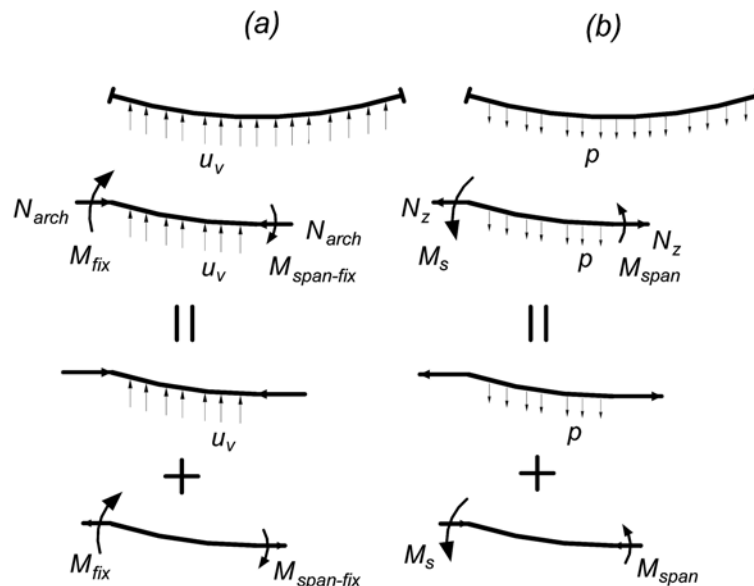


Fig. 7 Evaluation of compressive axial forces in inverted arch under live and prestressing loading

design purposes

$$M_{fix} = 200 \times u_v \times t^2 \quad (31)$$

whereas the corresponding bending moment $M_{span-fix}$ at the center of the span, causing tension to the upper fibres can be practically obtained from the expression

$$M_{span-fix} = 100 \times u_v \times t^2 \quad (32)$$

i.e., the half of the fixed-end moment M_{fix} .

The value M_{fix} must be superposed with M_s , resulting that way in a reduced bending response M_{s-fix} for the fixed end of the inverted arch. It is

$$M_{s-fix} = M_s + M_{fix} \quad (33)$$

The maximum positive bending response $M_{max-span}$ due to a live load p , can be obtained from the following relation

$$M_{max-span} = M_{span} - M_{span-fix} \quad (34)$$

However, for design purposes, the greater value M_{max} for a hinged girder may be used instead.

It has to be noted here that the occurring high compression forces do not imply a danger of snap-through buckling of the inverted arch, since the presence of the embedded high stressed cable, prevents this situation.

3. Design parameters and evaluation of response

At first it has to be noted that the live load p for a footbridge (in kN/m²), may be determined as a function of the span L (in m), according to the expression (Mehlhorn 2007)

$$p = 2.0 + \frac{120.0}{L + 30} \leq 5.0 \quad (35)$$

Introducing now the thinness ratio α and the prestressing reinforcement ratio ρ , according to the expressions

$$\alpha = \frac{t}{L}, \quad \rho = \frac{A_c}{b \cdot t} \quad (36)$$

as basic design parameters, the fictitious permanent load w and the uplift deviation load u_v due to prestressing, may then be expressed as follows

$$w = g + u_v = 8 \cdot \alpha \cdot \lambda \cdot \rho \cdot \sigma_{p0} \quad (37)$$

$$u_v = w - g = 8 \cdot \alpha \cdot \lambda \cdot \rho \cdot \sigma_{p0} - \gamma_c \cdot L \cdot \alpha \quad (38)$$

where $\gamma_c = 25 \text{ kN/m}^3$ represents the unit weight of concrete and σ_{p0} is the applied cable stress. Moreover it is obtained

$$H_w = \alpha \cdot \rho \cdot \sigma_{p0} \cdot L \quad (39)$$

$$H_v = \left(\sigma_{p0} \cdot \rho - \frac{\gamma_c \cdot L}{8 \cdot \lambda} \right) \cdot \alpha \cdot L \quad (40)$$

The three basic dimensionless parameters (15) can now be expressed as follows

$$G = \frac{12}{E_c \cdot \alpha^2} \cdot \sigma_{p0} \cdot \rho, \quad \gamma = \frac{p}{8 \cdot \alpha \cdot \lambda \cdot \rho \cdot \sigma_{p0}}, \quad \varepsilon = \frac{\sigma_{p0}}{E_0} \quad (41)$$

As already mentioned, the bending moments M_{max} and M_s can be deduced on the basis of the above three dimensionless parameters.

Regarding the compressive forces, in the case of a hinged inverted arch, the effective axial compressive force per unit width N_{c-hing} , may be obtained from the uplift pressure u_v and the live load p

$$N_{c-hing} = \frac{(u_v - p) \cdot L}{8 \cdot \lambda} \quad (42)$$

For the fixed inverted arch, the compressive force N_{d-fix} may be expressed as follows

$$N_{c-fix} = N_{arch} - N_z \quad (43)$$

In the above equation, N_{arch} represents the compressive force due to the uplift pressure u_v on the fixed arch (Fig. 7(a)). It may be written

$$N_{arch} = \frac{u_v \cdot L}{8 \cdot \lambda} - \frac{M_{fix} + M_{span-fix}}{\lambda \cdot L} \quad (44)$$

Besides in Eq. (43), N_z represents the tensile thrust due to the live load acting on the inverted arch, taking also into account the acting of bending moments M_s and M_{span} (Fig. 7(b)). It is obtained

$$N_z = \frac{p \cdot L}{8 \cdot \lambda} + \frac{M_s - M_{span}}{\lambda \cdot L} \quad (45)$$

(In Fig. 7 the bending and axial forces are shown in their physical sense)

It is now clear that in order to carry out the design of the orthogonal unit width section of the inverted arch in case of hinged supports, the pair of values (M_{max} and N_{d-hing}) referring to the middle of span must be used, whereas for the support section of the fixed arch the pair of values (M_s and N_{d-fix}) must be taken into account. For the middle of span the pair of values (M_{max} and N_{d-fix}) may be used according to what has been stated previously.

The total cable force H_{hing} or H_{fix} for the hinged or fixed arch case also has to be determined. It can be written respectively

$$H_{hing} = (1 + Z_{hing}) \cdot \rho \cdot \alpha \cdot \sigma_{p0} \cdot L \quad (46)$$

and

$$H_{fix} = (1 + Z_{fix}) \cdot \rho \cdot \alpha \cdot \sigma_{p0} \cdot L \quad (47)$$

where Z_{hing} and Z_{fix} correspond to the parameter Z determined in the case of hinged or fixed arch respectively, with the live load p extending over the whole span.

The above design magnitudes are based, as previously mentioned, on the assumption that no bond exists between the cable and the surrounding concrete ribbon. Consequently, they may be used

directly for preliminary design purposes, as they are lying on the safe side. Actually, the bond is established, if at all, after the cable prestressing has been performed.

4. Numerical procedure

For a stress-ribbon pedestrian bridge of span length L , with the selected design parameters α , ρ and for an assumed live load p according to Eq. (35), the analysis goes through the following steps, which can be directly performed by a computer program:

- Determination of w and u_v from Eqs. (37) and (38) respectively
- Determination of the dimensionless parameters from Eq. (41)

Hinged arch

1. Determination of the unknown parameter Z_{hing} according to Eq. (19).
2. Determination of M_{max} on the basis of Z_{hing} according to Eq. (21).
3. Determination of N_{c-hing} according to Eq. (42)
4. Determination of H_{hing} according to Eq. (46)

Fixed arch

1. Determination of the unknown parameter Z_{fix} , according to Eq. (27).
2. Determination of M_s and M_{span} on the basis of Z_{fix} , according to Eqs. (25) and (29).
3. Determination of M_{fix} and $M_{span-fix}$, from Eqs. (31) and (32).
4. Determination of M_{s-fix} and $M_{max-span}$ from Eqs. (33) and (34)
5. Determination of N_{c-fix} according to Eqs. (43), (44) and (45)
6. Determination of H_{fix} according to Eq. (47)

5. Design diagrams

The computer program written on the basis of the foregoing numerical procedure, not only allows a quick assessment of the response of a given prestressed ribbon pedestrian bridge, but also enables a parametric study of the problem in general.

As previously explained, the design is based on the following parameters :

Span length L , Shallowness ratio $\lambda = 0.02$, Thinness ratio α , Prestressing steel ratio ρ , Applied cable stress σ_{p0} , Concrete modulus of elasticity E_c , Modulus of elasticity E_0 of prestressing cable.

The diagrams of Figs. 8-23 show the influence of the span length L and the thinness ratio α , on the additional cable force, on the maximum bending response and on the effective corresponding normal force being caused by the live load of the pedestrian bridge. Both cases of fixed and hinged arch are examined and three values of the parameter ρ are considered, namely 0.015, 0.020 and 0.025. A pavement load equal to 1.0 kN/m² is taken also into account, being applied to the bridge after the prestressing is performed. In this investigation, the value $\sigma_{p0} = 960$ MPa is used, representing about 60% of the yield stress of the prestressing steel, whereas the values of E_c and E_0 are taken equal to 30000 MPa and 200000 Mpa, respectively.

From Figs. 8, 9 it can be seen that while in general the additional cable force increases linearly with the span length, in the hinged case it is completely independent from the thinness ratio, whereas in the fixed case it decreases slightly as this ratio increases. From this investigation it also comes out that the prestressing steel ratio does not practically influence the additional cable force.

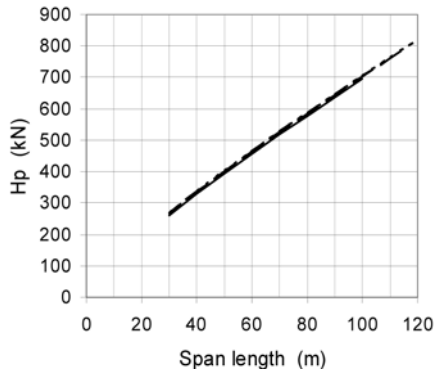


Fig. 8 Hinged arch. Additional cable force ($\rho = 0.025$)

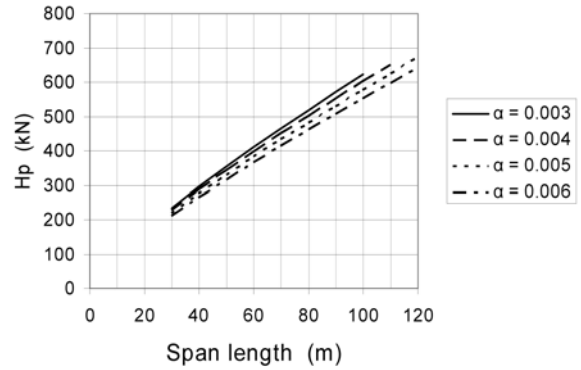


Fig. 9 Fixed arch. Additional cable force ($\rho = 0.025$)

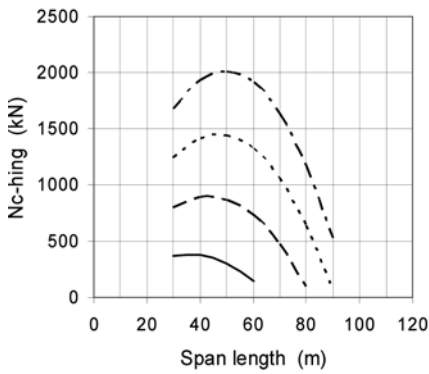


Fig. 10 Hinged arch. Axial compressive force ($\rho = 0.020$)

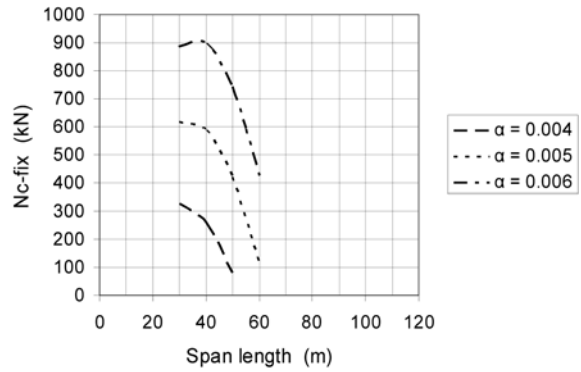


Fig. 11 Fixed arch. Axial compressive force ($\rho = 0.015$)

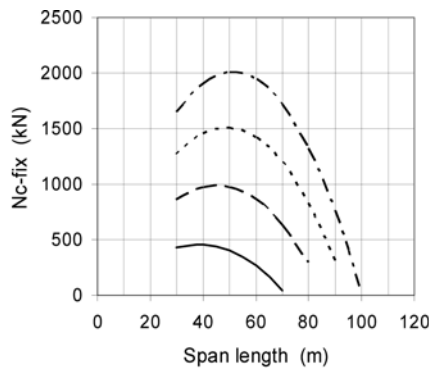


Fig. 12 Fixed arch. Axial compressive force ($\rho = 0.020$)

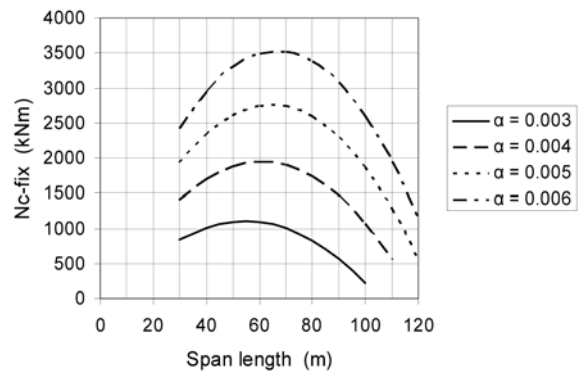


Fig. 13 Fixed arch. Axial compressive force ($\rho = 0.025$)

The variation of the axial compressive force is depicted in Figs. 10-13. It can be concluded that the values for both the fixed and the hinged case are practically the same.

As it may be seen, an increase of thinness ratio or of prestressing steel ratio, leads to a respective

increase of compressive force.

Regarding the maximum bending moment in the case of hinged arch, it is seen from Figs. 14-16, its value increases with the thinness ratio α , while it decreases with the prestressing steel ratio ρ . The bending moment values are very moderate and combined with the values of the corresponding high axial compression forces, lead to the conclusion that no tensile forces are developed in the

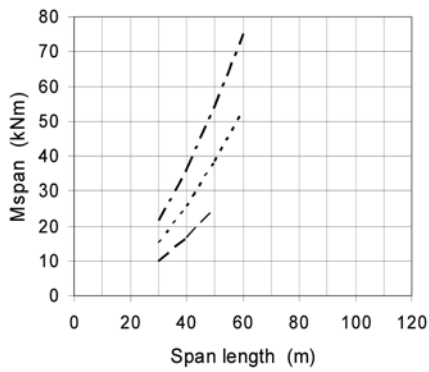


Fig. 14 Maximum span bending moment ($\rho = 0.015$)

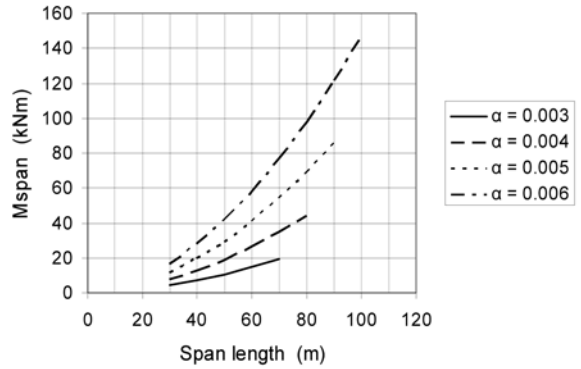


Fig. 15 Maximum span bending moment ($\rho = 0.020$)

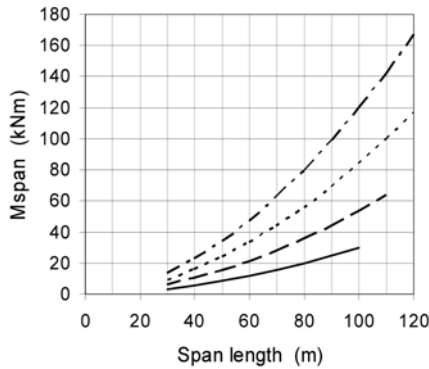


Fig. 16 Maximum span bending moment ($\rho = 0.025$)

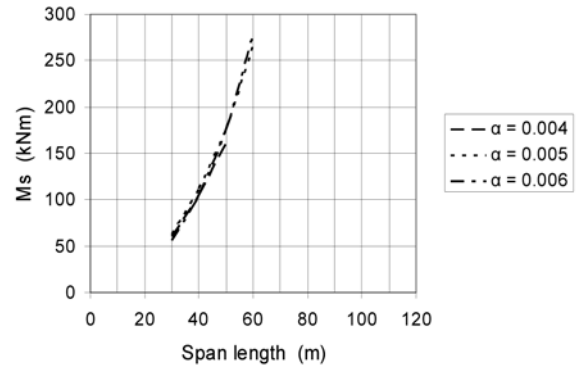


Fig. 17 Fixed-end bending moment ($\rho = 0.015$)

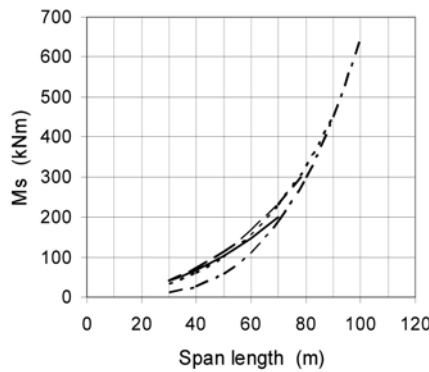


Fig. 18 Fixed-end bending moment ($\rho = 0.020$)

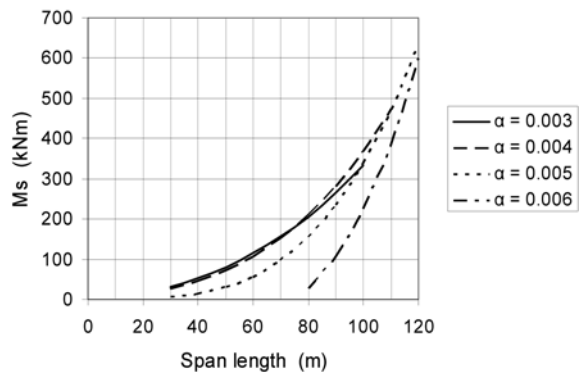


Fig. 19 Fixed-end bending moment ($\rho = 0.025$)

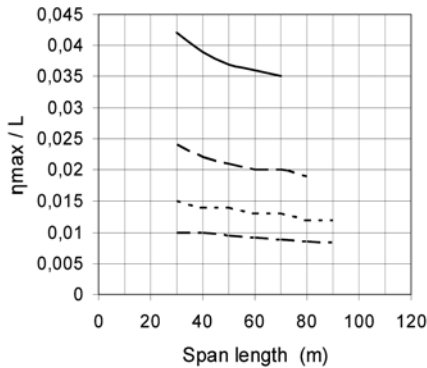


Fig. 20 Hinged arch. Maximum deflection ratio ($\rho = 0.020$)

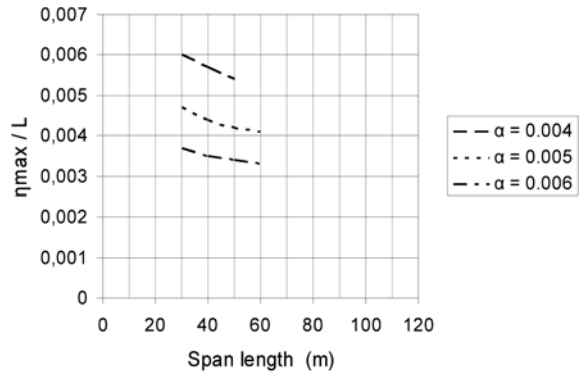


Fig. 21 Fixed arch. Maximum deflection ratio ($\rho = 0.015$)

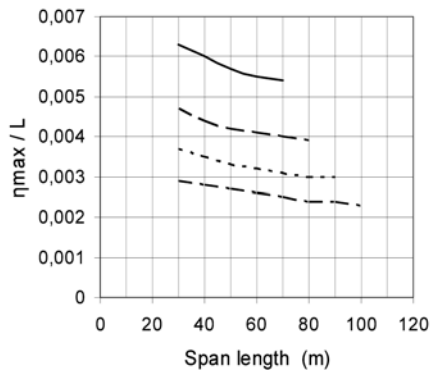


Fig. 22 Fixed arch. Maximum deflection ratio ($\rho = 0.020$)

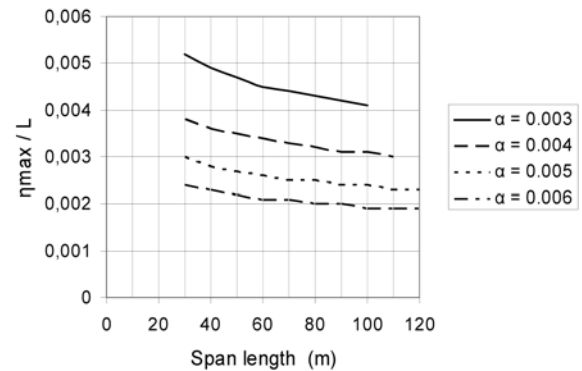


Fig. 23 Fixed arch. Maximum deflection ratio ($\rho = 0.025$)

orthogonal section of the inverted arch, as the resultant equivalent force acts always inside the core of that section. As previously stated, this bending moment may also be used as the design span moment for the fixed case.

The fixed-end bending moment as seen from Figs. 17-19, is more than six times greater than the span maximum moment and for that reason it represents the governing factor of the bending response in the design. It generally decreases with the increase of the prestressing steel ratio, whereas the thinness ratio does not particularly affect its value.

Taking into account the prevailing compressive forces from the above Figs. 13-15, it can be directly concluded that the bending response in the supports requires a respective reinforcement in the section.

Finally, as it can be seen from Figs. 20-23, the maximum deflection ratio (η/L) decreases with an increase of both the thinness and the prestressing steel ratio,. However, the high values of deflection ratio of hinged arches in comparison to those of the fixed arches, make their use as pedestrian bridges problematic, as this has been previously pointed out.

From all the above diagrams it can be generally concluded that, increase of span length leads to a selection of a higher thinness ratio and a prestressing steel ratio too.

6. Numerical example

A ribbon bridge with a span of 60 m and a thickness of 22 cm, fixed at its both ends, is considered. For a prestressing arrangement corresponding to the selected thickness according to the prestressing system BBRV, the area of 4235 mm² of prestressing steel is selected. From the above data, the thinness ratio and the prestressing steel ratio are obtained, as $\alpha = 0.00367$ and $\rho = 0.01925$ respectively. The live load according to Eq. (35), is equal to $p = 3.33$ kN/m². Moreover, a pavement load equal to 1.0 kN/m² is considered, which may be added to the live load, as this is brought on the bridge after the prestressing of the ribbon is performed.

The numerical procedure described above leads to the following results, all referring to a unit width (1 m) of the bridge:

Fictitious load $w = 10.84$ kN/m

Uplift prestressing pressure $u_v = 5.34$ kN/m

Initial cable force due to concrete weight and prestressing : $H_w = 4065.60$ kN

The unknown parameter Z of the problem results equal to 0.0954 and the additional cable force H_p due to live load is obtained as $H_p = 0.0954 \times 4065.60 = 387.85$ kN, leading to a total cable force $H_{fix} = 4453.50$ kN and a total cable stress equal to 1051594 kN/m².

The resulting bending moment and corresponding compressive force at the end sections of the inverted arch are : $M_{s-fix} = 170.53$ kNm (tension of upper fibers) and

$N_{c-fix} = 515.09$ kN (compression) respectively. This response requires an additional reinforcement of $\Phi 25 / 15$ and $\Phi 18 / 15$, on the top and bottom side respectively.

For the maximum bending moment in the span, the resulting maximum bending response M_{max} of the hinged arch may be used, as previously mentioned. It is obtained :

$M_{max} = 22.86$ kNm, whereas the acting compressive normal force is : $N_{d-hing} = 378.10$ kN

Although the last pair of values excludes the development of tensile stresses in the section, a minimum reinforcement of $\Phi 10/15$ has to be placed both at the top and bottom side.

7. Conclusions

The static response of a prestressed-ribbon concrete pedestrian bridge under live load, can be obtained directly through a corresponding suspended beam model, using only two dimensionless design parameters, namely the ratio of the thickness over the span length and the ratio of the prestressing steel area over the concrete section area. The preliminary design can be performed directly, using comprehensive parametric diagrams, which allow the determination of all the relevant magnitudes. The design is governed by the bending response at the fixed end of the bridge, where additional reinforcement is needed. The unusually restricted concrete thickness, although environmentally and aesthetically satisfying, requires a relatively high percentage of prestressing steel, particularly as the span length of the bridge increases.

References

- Arco, D.C., Aparicio, A.C. and Mari, A.R. (2001), "Preliminary design of prestressed concrete stress ribbon bridge", *J. Bridge Eng.*, **6**(4), 234-242.

- Mehlhorn, G. (2007), "Handbook – Bridges", Springer, Berlin, New York (in German).
- Redfield, C. and Strasky, J. (1991), "Sacramento river pedestrian bridge, USA", *Struct. Eng. Int.*, **1**(4), 19-21.
- Schlaich, J. and Engelsmann, S. (1996), "Stress ribbon concrete bridges", *Struct. Eng. Int.*, **6**(4), 271-274.
- Stavridis, L.T. (2008), "A simplified analysis of the behavior of suspension bridges under live load", *Struct. Eng. Mech.*, **30**(5), 559-576.
- Timoshenko, S. (1956), *Strength of Materials Part II*, D. Van Nostrand Company Inc., New York.